Ultrafast Generation of Pseudo-magnetic Field for Valley Excitons in WSe2 Monolayers

Authors: Jonghwan Kim[†,1], Xiaoping Hong[†,1], Chenhao Jin[1], Su-Fei Shi[1,2], Chih-Yuan S. Chang[3], Ming-Hui Chiu[4], Lain-Jong Li[3,4], Feng Wang[1,2,5*]

Affiliations:

[1] Department of Physics, University of California at Berkeley, Berkeley, CA 94720, United States.

[2] Material Science Division, Lawrence Berkeley National Laboratory, Berkeley, CA, 94720, United States.

[3] Institute of Atomic and Molecular Sciences, Academia Sinica, Taipei 10617, Taiwan.

[4] Physical Sciences and Engineering, King Abdullah University of Science and Technology, Thuwal, Saudi Arabia.

[5] Kavli Energy NanoSciences Institute at University of California Berkeley and Lawrence Berkeley National Laboratory, Berkeley, CA 94720, United States.

* Correspondence to: fengwang76@berkeley.edu

† These authors contribute equally to this work

Abstract:

The valley pseudospin is a degree of freedom that emerges in atomically thin two-dimensional transition metal dichalcogenides (MX_2). The capability to manipulate it in analogy to the control of spin in spintronics can open up exciting opportunities. Here we demonstrate that an ultrafast and ultrahigh valley pseudo-magnetic field can be generated using circularly polarized femtosecond pulses to selectively control the valley degree of freedom in monolayer MX_2. Employing ultrafast pump-probe spectroscopy, we observed a pure and valley-selective optical Stark effect in WSe_2 monolayers from the non-resonant pump, resulting in an energy splitting of more than 10 meV between the K and K' valley exciton transitions. Our study opens up the possibility to coherently manipulate the valley polarization for quantum information applications.

Main Text:

Atomically thin layers of transition metal dichalcogenides (MX_2) have emerged as an exciting two-dimensional semiconductor platform for nanoelectronics and optoelectronics(*1, 2*). In particular, a pair of degenerate bands are present at the K and K' valleys in the momentum space of hexagonal MX_2 monolayers, giving rise to a unique valley degree of freedom that is analogous to electron spin(*3*). Recent polarization-resolved photoluminescence (PL) studies show that the valley pseudospin in MX_2 can couple directly to the helicity of excitation photons(*4-7*), and that the pseudospin polarization between two valleys exhibits coherent

behavior(*7*). It raises the intriguing prospect of valleytronics, which exploits the valley degree of freedom to carry information(*1, 3-9*).

Just as spin manipulation in spintronics, the capability to control the valley pseudospin is essential for valleytronics based on MX_2 materials. In spintronics, the electron spin can be manipulated through any external perturbation that breaks the energy degeneracy of two orthogonal spin polarizations. This can be achieved either through an external magnetic field (*10, 11*), or through a pseudo-magnetic field generated by other stimuli. For example, circularly polarized light can produce a pseudo-magnetic field that can be used to manipulate electron spins in semiconductor quantum wells and quantum dots (*12, 13*) through the optical Stark effect. (The optical Stark effect, a well-established phenomenon in atomic physics and quantum optics, describes the energy shift in a two-level system induced by a non-resonant laser field.) It is highly desirable to realize similar control of valley excitons in MX_2 using light-induced pseudo-magnetic field for valleytronics.

Here we demonstrate a valley-selective optical Stark effect in monolayer WSe_2 to generate ultrafast and ultrahigh pseudo-magnetic field for valley excitons. Previously, resonant pump-probe spectroscopy has been used to probe ultrafast carrier dynamics after the pump photons are absorbed by exciton transitions in MX_2 monolayers(*14-17*). Here we use non-resonant circularly polarized laser pumping with photon energies below the bandgap, which induces a coherent and dissipationless valley-selective optical Stark effect for pseudospin manipulation.

We used triangular monolayers of WSe_2 grown by chemical vapor deposition on sapphire substrates(*18*) (Fig. 1A, inset). The optical reflection spectrum of monolayer WSe_2 at 77 K exhibits two prominent resonances at 1.68 eV and 2.1 eV (Fig. 1A), which correspond, respectively, to the A- and B- excitons split by the spin-orbital coupling (*19, 20*). In this study, we focused on the lowest energy A-exciton transition. This A-exciton is well separated from other excited states in energy thanks to strong electron-hole interactions in monolayer WSe_2. As a result, we can approximate the ground state and the A-exciton as a two-level system and neglect the effect from other excited states. In monolayer WSe_2 the A-exciton states at K and K' valleys are time-reversal pairs and have degenerate energy levels. However, they have distinct optical selection rules and couple to photons of opposite helicity (*3, 4*). The dipole transition

matrix element of the K-valley A-exciton is characterized by $P_K^{\sigma\pm} = \langle K|\hat{p}_x \pm i\hat{p}_y|0\rangle$, where $|K\rangle$ and $|0\rangle$ correspond to the K-valley A-exciton and ground state, respectively, $\hat{p}_x, \hat{p}_y$ are momentum operators, and σ_+ / σ_- corresponds to left/right circular light. In MX$_2$ monolayers $P_K^{\sigma+}$ has a finite value but $P_K^{\sigma-}$ is approximately zero. Consequently, the A-exciton at the K valley couples exclusively to left-circularly polarized light. The A-exciton at the K' valley, on the other hand, couples only to the right-circularly polarized light. This dipole selection rule for valley transitions in monolayer WSe$_2$ governs both resonant and non-resonant excitations, which can have different manifestations in valley physics.

The valley-dependent resonant excitation enables both the generation of a valley-polarized exciton population through the absorption of circularly polarized light and the detection of valley-polarized excitons through polarization-resolved photoluminescence (PL)(*4-6*). Figure 1B displays polarization-resolved PL spectra of our WSe$_2$ samples upon laser excitation at 1.8 eV with σ_+ circular polarization, where the PL intensity with helicity matching the excitation light (σ_+, red curve) is about four times stronger than that for the opposite helicity (σ_-, blue curve). This behavior is similar to that reported in previous studies(*4-7*), and verifies the valley-selective excitation and emission in our WSe$_2$ monolayers. The non-zero σ_- polarized PL is presumably caused by a finite intervalley scattering because the excitation energy is ~120 meV higher than the A-exciton resonance.

To manipulate the valley polarization, however, non-resonant coupling based on the optical Stark effect is more advantageous because it avoids the dissipation and dephasing naturally accompanying real excitations. The optical Stark effect is widely used in quantum optics to control a rich variety of quantum systems, ranging from the manipulation of cold atoms (*21*) and individual trapped ions (*22*) to coherent control of superconducting qubits (*23*) and electron spins (*24*). In a two-level system, the optical Stark effect can be readily understood using the dressed atom picture(*25*). Consider the two-level system composed of the ground state and A-exciton state at the K (or K') valley in a monolayer WSe$_2$. Figure 2A illustrates the effect of a left circularly polarized (σ_+) pump with photon energies below the exciton resonance (red arrow). In the dressed atom picture, the dressed ground state (with N σ_+ photons) and the K-valley A-exciton (with N-1 σ_+ photons) are coupled by the dipole transition, which leads to wavefunction hybridization and energy level repulsion. It effectively shifts down the ground

state energy and shifts up the K-valley exciton energy. The A-exciton at the K' valley, on the other hand, cannot couple to the ground state with an extra σ_+ photon because of the optical selection rule, and the related states are not shifted by σ_+ polarized light. As a result, the energy degeneracy between K and K' valley states is lifted by the valley-selective optical Stark effect, which can be characterized by a valley pseudo-magnetic field.

We measured the valley-selective optical Stark shift in WSe$_2$ monolayers with non-resonant circularly polarized excitation using pump-probe spectroscopy. Femtosecond pump pulses with tunable photon energies below the A-exciton resonance were generated by an optical parametric amplifier. Optical Stark shifts of the WSe$_2$ exciton transitions induced by the pump pulses was then probed in transient reflection spectra over the spectral range of 1.59-1.77 eV using a laser-generated supercontinuum light. Figure 2B and 2C display two-dimensional plots of transient reflection spectra in a monolayer WSe$_2$ with σ_+ and σ_- polarized probe light, respectively, upon σ_+ polarized pump excitation. Here the non-resonant pump photons are at 1.53 eV, which is 150 meV below the exciton resonance and do not excite any real transitions. The color scale in Fig. 2B and 2C represents the pump-induced change of the probe beam reflectivity $\Delta R/R$, the horizontal axis shows the probe photon energy, and the vertical axis shows the pump-probe time delay. For atomically thin WSe$_2$ layers on a transparent sapphire substrate, the reflection change $\Delta R/R$ is directly proportional to the change in the absorption coefficient(*26, 27*). It is apparent that strong changes in the exciton absorption are present only for σ_+ probe pulses (Fig. 2B), and no pump-induced signals can be detected above the noise level for σ_- probe pulses (Fig. 2C). This indicates that the non-resonant σ_+ pump significantly modifies the A-exciton transition at the K valley, but not at the K' valley.

To better examine the time evolution and spectral lineshape of the photo-induced transient reflection spectra in WSe$_2$ monolayers, we plot in Fig. 3 vertical and horizontal linecuts of the two-dimensional plot for the σ_+ pump and σ_+ probe configuration (Fig. 2B). Figure 3A displays the transient reflection signals at the probe photon energy below (1.65 eV, blue line) and above (1.7 eV, red line) the exciton resonance at different pump-probe delay τ (vertical linecuts in Fig. 2B). Both signals have the largest magnitude at τ=0 and show a symmetric rise and decay dynamics. This is characteristic of an instantaneous response with the rise/decay time limited by the laser pulse width of ~ 250 fs. It shows that the exciton absorption is modulated only when the

pump radiation is present. In addition, the transient reflectivity has opposite signs for probe energies at 1.65eV and 1.7 eV. Detailed transient reflection spectrum $\Delta R/R$, which is proportional to the transient absorption change(*26, 27*), is shown in Fig. 3B (green circles) for τ=0 through a horizontal linecut in Fig. 2B. We observe that the transient absorption signal changes sign at exactly at the A-exciton resonance energy E_A=1.68 eV. The pump laser leads to reduced absorption below E_A and increased absorption above E_A, which matches well the linear derivative of the WSe$_2$ monolayer absorption spectrum (magenta line in Fig. 3B). Quantitatively, the photo-induced absorption change can be perfectly described by a simple blueshift of ~ 4 meV of the K-valley exciton resonance. The blueshift in transition energy, instantaneous time response, and valley selectivity demonstrate unambiguously the optical Stark effect in monolayer WSe$_2$ upon non-resonant pump excitation. We note that the photo-induced signal becomes non-detectable immediately after the pump pulses, indicating negligible dissipative processes associated with real exciton absorption. We also performed the pump-probe spectroscopy using linearly polarized pump and probe pulses (Fig. S1). Here photo-induced absorption changes are of similar magnitude independent of the pump and probe polarizations. This is because the linear-polarized pump has both σ_+ and σ_- components, which lead to optical Stark shifts for both K and K' valley exciton transitions.

Next we examine how the valley-selective optical Stark shift varies with the pump laser intensity and detuning. The pump detuning $\hbar\Omega$ is defined as the difference between the exciton resonance energy ($\hbar\omega_0$) and the pump photon energy ($\hbar\omega_p$). Figure 4 shows the transient reflection data (left axis) and the corresponding energy shift of the A-exciton energy (right axis, supplementary online text) at the K valley for σ_+ pump and σ_+ probe configuration with different pump detuning (green dots in Fig. 4A) and pump intensities (green dots in Fig. 4B). We observe that the optical Stark shift is inversely proportional to the pump detuning (magenta dashed line in Fig. 4A), and scales linearly with the laser intensity (magenta dashed line in Fig. 4B). Such scaling matches well with the theoretical prediction of optical Stark shift $\delta(\hbar\omega_0) = 2S \cdot E_p^2/\hbar\Omega$, where S is the optical Stark shift constant related to the transition dipole moment and E_p is the electric field of the pump pulse(*25, 28*). From the experimental data, we can determine an optical Stark shift constant S ~ 45 Debye^2 for A-exciton in monolayer WSe$_2$, which is of similar

magnitude to that for exciton transition in semiconductor quantum wells(*29*).

The valley-selective optical Stark shift breaks the degeneracy of valley exciton transitions in monolayer WSe$_2$ and defines an effective valley pseudo-magnetic field. In our experiment, the photo-induced energy splitting between K and K' exciton transitions can be as large as 10 meV (Fig. 4 and supplementary online text). The corresponding pseudo-magnetic field B$_{eff}$ for valley excitons can be estimated by $B_{eff} = \frac{\Delta E}{2g_{ex}\mu_B}$, where μ_B is the Bohr magneton and g$_{ex}$ is the effective g-factor for valley exciton transitions in WSe$_2$. The effective exciton g-factor g$_{ex}$ combines contributions from both electrons and holes, and has a theoretically predicted value ~ 1.5 for WSe$_2$ (supplementary online text). Using this g-factor, we estimate a pseudo-magnetic field B$_{eff}$ as high as 60 T for a 10 meV splitting of valley exciton transitions. A real magnetic field of this magnitude is difficult to achieve even with superconducting magnets, but such a pseudo-magnetic field for MX$_2$ valley excitons can be produced conveniently and with femtosecond temporal control using light pulses.

It has been reported recently that excitons in different valleys in monolayer WSe$_2$, resonantly excited by linear polarization light can maintain their phase coherence over extended time (*7*). The valley-dependent optical Stark effect offers a convenient and ultrafast way to lift the valley degeneracy and introduce a controlled phase difference between the two valley states, therefore enabling coherent rotation of resonantly excited valley polarizations with high fidelity (Fig. S2). In analogy with spintronics, such coherent manipulation of valley polarization can open up fascinating opportunities for valleytronics.

References:

1.	X. Xu, W. Yao, D. Xiao, T. F. Heinz, Spin and pseudospins in layered transition metal dichalcogenides. *Nat Phys* **10**, 343 (2014).
2.	Q. H. Wang, K. Kalantar-Zadeh, A. Kis, J. N. Coleman, M. S. Strano, Electronics and optoelectronics of two-dimensional transition metal dichalcogenides. *Nature Nanotechnology* **7**, 699 (2012).

3. D. Xiao, G. B. Liu, W. X. Feng, X. D. Xu, W. Yao, Coupled Spin and Valley Physics in Monolayers of MoS2 and Other Group-VI Dichalcogenides. *Physical Review Letters* **108**, (2012).

4. T. Cao *et al.*, Valley-selective circular dichroism of monolayer molybdenum disulphide. *Nature Communications* **3**, (2012).

5. K. F. Mak, K. L. He, J. Shan, T. F. Heinz, Control of valley polarization in monolayer MoS2 by optical helicity. *Nature Nanotechnology* **7**, 494 (2012).

6. H. L. Zeng, J. F. Dai, W. Yao, D. Xiao, X. D. Cui, Valley polarization in MoS2 monolayers by optical pumping. *Nature Nanotechnology* **7**, 490 (2012).

7. A. M. Jones *et al.*, Optical generation of excitonic valley coherence in monolayer WSe2. *Nature Nanotechnology* **8**, 634 (2013).

8. Y. J. Zhang, T. Oka, R. Suzuki, J. T. Ye, Y. Iwasa, Electrically Switchable Chiral Light-Emitting Transistor. *Science* **344**, 725 (2014).

9. K. F. Mak, K. L. McGill, J. Park, P. L. McEuen, The valley Hall effect in MoS2 transistors. *Science* **344**, 1489 (2014).

10. C. P. Poole, Electron spin resonance 2nd edn, Wiley New York (1983)

11. F. H. L. Koppens *et al.*, Driven coherent oscillations of a single electron spin in a quantum dot. *Nature* **442**, 766 (2006).

12. J. A. Gupta, R. Knobel, N. Samarth, D. D. Awschalom, Ultrafast manipulation of electron spin coherence. *Science* **292**, 2458 (2001).

13. D. Press, T. D. Ladd, B. Y. Zhang, Y. Yamamoto, Complete quantum control of a single quantum dot spin using ultrafast optical pulses. *Nature* **456**, 218 (2008).

14. H. Shi *et al.*, Exciton Dynamics in Suspended Monolayer and Few-Layer MoS2 2D Crystals. *ACS Nano* **7**, 1072 (2012).

15. Q. Wang *et al.*, Valley Carrier Dynamics in Monolayer Molybdenum Disulfide from Helicity-Resolved Ultrafast Pump–Probe Spectroscopy. *ACS Nano* **7**, 11087 (2013).

16. E. J. Sie, Y.-H. Lee, A. J. Frenzel, J. Kong, N. Gedik, Biexciton formation in monolayer MoS2 observed by transient absorption spectroscopy. *arXiv:1312.2918*, (2013).

17. C. Mai *et al.*, Many-Body Effects in Valleytronics: Direct Measurement of Valley Lifetimes in Single-Layer MoS2. *Nano Letters* **14**, 202 (2013).

18.	J.-K. Huang *et al.*, Large-Area Synthesis of Highly Crystalline WSe2 Monolayers and Device Applications. *ACS Nano* **8**, 923 (2013).

19.	A. Splendiani *et al.*, Emerging Photoluminescence in Monolayer MoS2. *Nano Letters* **10**, 1271 (2010).

20.	K. F. Mak, C. Lee, J. Hone, J. Shan, T. F. Heinz, Atomically thin MoS 2: a new direct-gap semiconductor. *Physical Review Letters* **105**, 136805 (2010).

21.	P. Jessen, I. Deutsch, Optical lattices. *Adv. At. Mol. Opt. Phys* **37**, 95 (1996).

22.	C. Cohen-Tannoudji, Manipulating atoms with photons. *Physica Scripta* **1998**, 33 (1998).

23.	D. I. Schuster *et al.*, ac Stark Shift and Dephasing of a Superconducting Qubit Strongly Coupled to a Cavity Field. *Physical Review Letters* **94**, 123602 (2005).

24.	J. Berezovsky, M. H. Mikkelsen, N. G. Stoltz, L. A. Coldren, D. D. Awschalom, Picosecond coherent optical manipulation of a single electron spin in a quantum dot. *Science* **320**, 349 (2008).

25.	C. Cohentannoudji, S. Reynaud, Dressed-atom description of resonance fluorescence and absorption-spectra of a multilevel atom in an intense laser-beam. *Journal of Physics B-Atomic Molecular and Optical Physics* **10**, 345 (1977).

26.	F. Wang *et al.*, Gate-variable optical transitions in graphene. *Science* **320**, 206 (2008).

27.	K. F. Mak *et al.*, Measurement of the Optical Conductivity of Graphene. *Physical Review Letters* **101**, (2008).

28.	Y.-R. Shen, The principles of nonlinear optics. *New York, Wiley-Interscience* (1984).

29.	A. Von Lehmen, D. S. Chemla, J. P. Heritage, J. E. Zucker, Optical Stark effect on excitons in GaAs quantum wells. *Opt. Lett.* **11**, 609 (1986).

30.	H. Rostami, A. G. Moghaddam, R. Asgari, Effective lattice Hamiltonian for monolayer MoS2: Tailoring electronic structure with perpendicular electric and magnetic fields, Phys. Rev. B **88**, 085440 (2013).

31	H. Shi, H. Pan, Y.-W. Zhang, B. I. Yakobson, Quasiparticle band structures and optical properties of strained monolayer MoS2 and WS2, Phys. Rev. B **87**, 155304 (2013).

32	G. Aivazian et al., Magnetic Control of Valley Pseudospin in Monolayer WSe2. arXiv:1407.2645 (2014)

33	A. Srivastava et al., Valley Zeeman Effect in Elementary Optical Excitations of a Monolayer WSe2. arXiv:1407.2624 (2014).

34   D. MacNeill et al., Valley degeneracy breaking by magnetic field in monolayer MoSe2. arXiv:1407.0686] (2014).
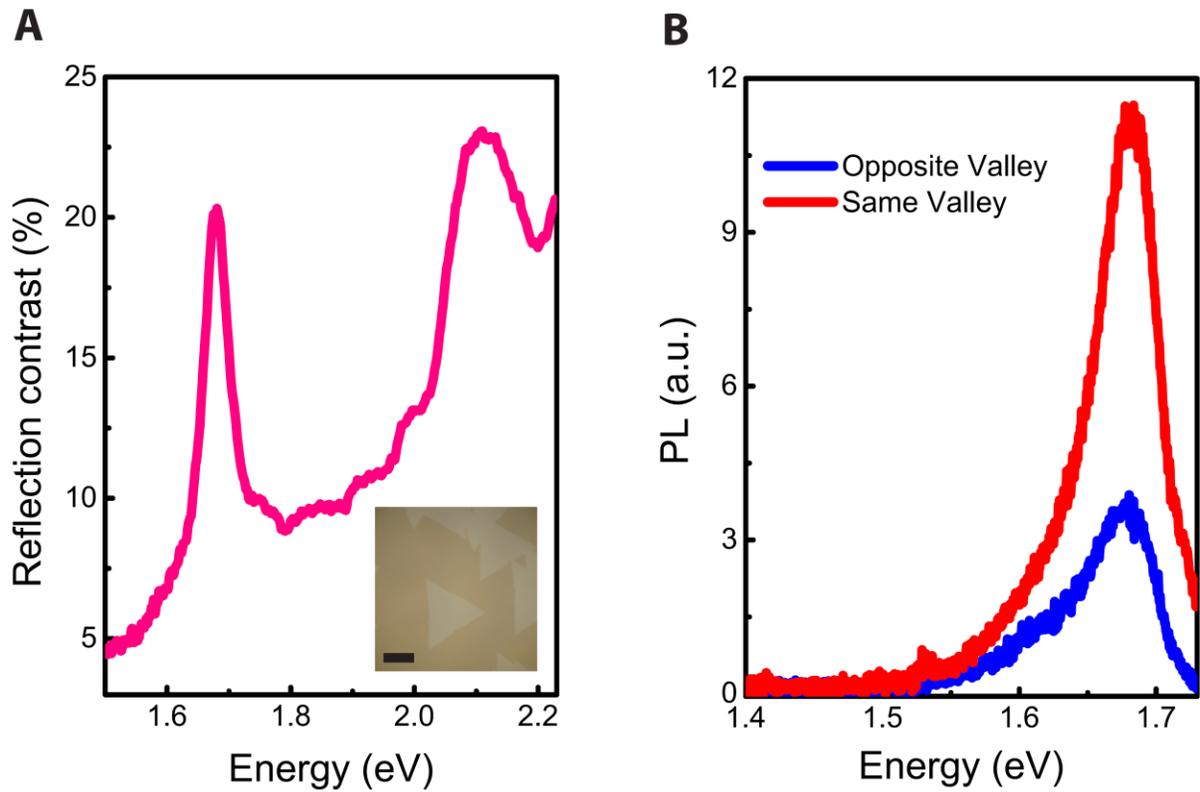
Fig. 1: Valley exciton transitions in monolayer WSe₂. (A) The optical reflection spectrum of a WSe₂ monolayer on a sapphire substrate at 77 K, which exhibit strong A- and B-exciton resonances at 1.68 eV and 2.1 eV, respectively. The inset shows optical microscopy image of the sample. The scale bar corresponds to 25 μm. **(B)** Polarization-resolved PL spectra of a WSe₂ monolayer at 77K. For 1.8 eV excitation laser with left circular polarization, the PL spectra show a prominent emission peak at the A-exciton resonance (1.68 eV), and the PL intensity with left circular polarization (red curve) is about four times stronger than that with right circular polarization (blue curve). It demonstrates that valley-polarized A-exciton population can be created by circularly polarized resonant excitation, and it can be detected by polarization-resolved PL spectroscopy.
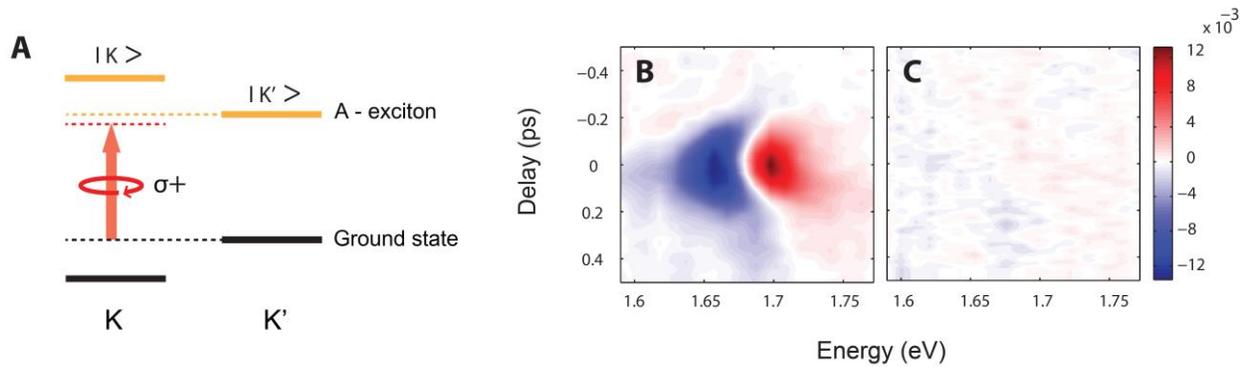
Fig. 2: Valley-dependent optical Stark effect with non-resonant circularly polarized pump.
(A) Schematic illustration of the optical Stark effect for valley transitions with non-resonant, left circularly polarized σ_+ pump. The dashed black and yellow lines denote the unperturbed ground and exciton states, respectively, and the pump photon energy is lower than the exciton resonance energy (red arrow). In the dressed atom picture, the dressed ground state (with N σ_+ photons) and the K-valley A-exciton (with N-1 σ_+ photons) are coupled by dipole transition, which results in energy level repulsion (solid black and yellow lines on the left section) and an increased exciton transition energy. On the other hand, σ_+ pump does not affect K'-valley A-exciton resonance due to optical selection rule (right section). **(B) and (C)** Transient reflection spectra of A-exciton resonance at 77 K. The colour scale, horizontal axis, and vertical axis represent the relative reflectivity change $\Delta R/R$, the probe photon energy, and the pump-probe time delay, respectively. For atomically thin WSe_2 on sapphire substrate, $\Delta R/R$ is proportional to absorption change. Non-resonant σ_+ pump of photon energy at 1.53 eV leads to a strong transient absorption signal for probes with the same polarization σ_+ **(B),** but produces no transient response for probes with the opposite polarization σ_- **(C)**. It demonstrates that non-resonant σ_+ pump significantly modifies A-exciton transition at the K valley, but not at the K' valley.
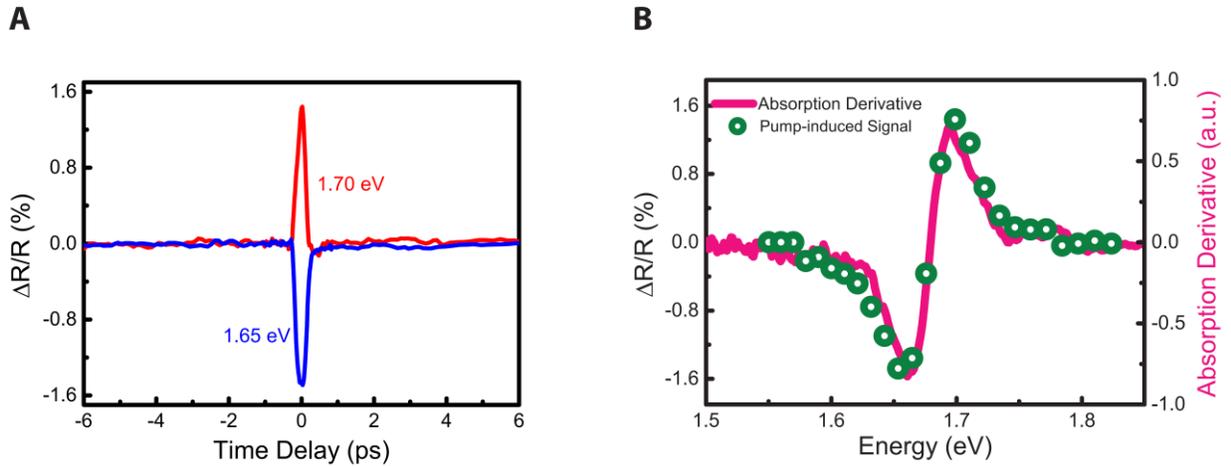
Fig. 3: Time evolution and spectral lineshape of the valley-dependent transient reflection spectra for σ_+ pump and σ_+ probe configuration. **(A)** Time evolution of the pump-induced transient reflectivity $\Delta R/R$ at probe energies of 1.65 eV (blue line) and 1.7 eV (red line). Both signals reach the maximum magnitude at the pump-probe delay $\tau=0$ with symmetric rise and decay dynamics (limited by our pulse width ~250 fs), which is characteristic of an instantaneous optical response. The transient reflectivity has opposite signs for 1.65 eV and 1.7 eV probes. **(B)** The transient reflection spectrum at $\tau=0$ (green circles). The transient reflectivity signal changes sign at the A-exciton resonance energy E_A=1.68 eV, and it shows a dispersive line shape. This transient reflection spectrum matches well with the derivative of linear absorption spectrum in monolayer WSe$_2$, and can be fully accounted for by a 4 meV blueshift of the K-valley A-exciton resonance (magenta line).
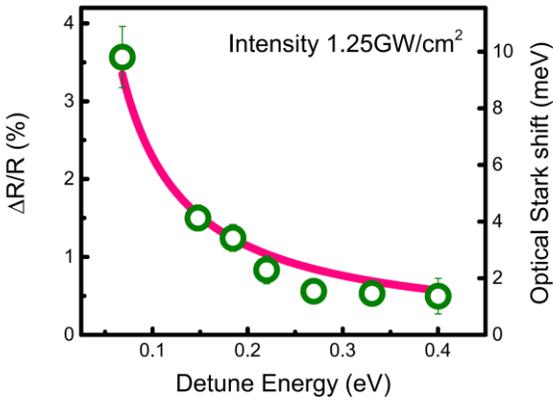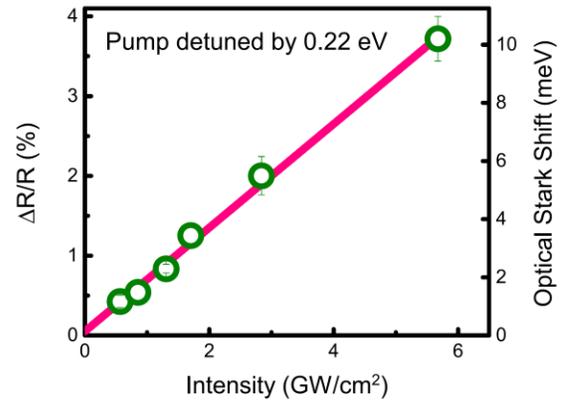
Fig. 4: Pump detuning and pump intensity dependence of the valley-selective optical Stark shift. **(A)** The transient reflection signal at 1.7 eV (left axis) and the corresponding optical Stark shift (right axis) as a function of the pump detuning energy (green dots). The dependence can be nicely described by an inverse proportional relationship (magenta line). **(B)** The transient reflection signal at 1.7 eV (left axis) and the corresponding optical Stark shift (right axis) as a function of the pump laser intensity (green dots), which shows a linear scaling behavior (magenta line). The optical Stark shift can selectively shift the K-valley exciton transition by as much as 10 meV, which corresponds to a valley pseudo-magnetic field of ~ 60 T.